

Euclidean Weak-Field General Relativity on the Lattice

C. Bouchard*

*University of Glasgow,
Glasgow, UK*

E-mail: chris.bouchard@glasgow.ac.uk

A lattice formulation of Euclidean, weak-field, path integral quantized general relativity – the low energy effective theory of quantum gravity – is presented. The lattice formulation allows the generation of a Markov chain of dynamic, vacuum (matter free) spacetimes at non-zero temperature, obtained here using the Metropolis algorithm. The positive action conjecture is implemented on the lattice, ensuring both a probabilistic interpretation of $\exp(-S_{\text{GR}})$ and that $\delta(S_{\text{GR}}) = 0$ generates the Einstein field equations. Equilibrated spacetimes are found to have nonzero curvature, a consequence of quantization. Preliminary studies of discretization and finite volume systematic effects, and the variation of vacuum spacetime curvature with temperature are presented. Prospects and future directions, including the combination with the QCD vacuum, are discussed.

*The 40th International Symposium on Lattice Field Theory (Lattice 2023)
July 31st - August 4th, 2023
Fermi National Accelerator Laboratory*

*Speaker

1. Euclidean, path integral quantized, weak-field general relativity

Neglecting a cosmological constant, the general relativistic (GR) action and path integral are

$$S_{\text{GR}} = \int d^4x \kappa \sqrt{-\det \mathbf{g}} R, \quad Z = \int d[\mathbf{g}] e^{iS_{\text{GR}}(\mathbf{g})}, \quad (1)$$

where $\kappa = c^4/16\pi G \sim 10^{35} \text{ fm}^{-2}$.¹ Wick rotation $t \rightarrow -it_{\text{E}}$, or equivalently complexifying the metric $\sqrt{-\det \mathbf{g}} \rightarrow -i\sqrt{\det \mathbf{g}_{\text{E}}}$, and identifying $S_{\text{GR}} \rightarrow iS_{\text{GR,E}}$ gives

$$S_{\text{GR}} = - \int d^4x \kappa \sqrt{\det \mathbf{g}} R, \quad Z = \int d[\mathbf{g}] e^{-S_{\text{GR}}(\mathbf{g})}, \quad (2)$$

where we drop the subscript E and work exclusively with Euclidean metric. In the weak-field regime and using the background field method [1], the dynamic small field $\mathbf{h}(x)$ lives on a static flat background spacetime with metric $\boldsymbol{\eta} = \text{diag}(1, 1, 1, 1)$, so that

$$g_{\mu\nu}(x) = \eta_{\mu\nu} + h_{\mu\nu}(x), \quad |h_{\mu\nu}| \ll 1. \quad (3)$$

Because \mathbf{h} lives on flat spacetime, a simple Wick rotation suffices and we avoid issues associated with complex metric [2]. There is no distinction between upper and lower indices and we use lower throughout. At $\mathcal{O}(h)$, $\sqrt{\det \mathbf{g}} R$ is a total derivative whose integral vanishes due to boundary constraints discussed in Sec. 3. The leading contribution to \mathcal{L}_{GR} is then $\mathcal{O}(h^2)$ [1],

$$\mathcal{L}_{\text{GR}}^{(2)} = \frac{\kappa}{2} \left(\frac{1}{2} (\partial_\rho h_{\mu\nu})^2 - \frac{1}{2} (\partial_\mu \text{tr} \mathbf{h})^2 + \partial_\nu h_{\mu\nu} \partial_\mu \text{tr} \mathbf{h} - \partial_\rho h_{\mu\nu} \partial_\nu h_{\rho\mu} \right). \quad (4)$$

Some historical context: The path integral was proposed in [3] as an approach to quantum gravity then later revived with Euclidean metric (see the collected works in [4]), which required ensuring $S_{\text{GR}} \geq 0$ via the positive action conjecture [5–8]. Though nonrenormalizability [1, 9] moved the search for a UV completion elsewhere, this can be seen as a simple consequence of an effective field theory description of the UV theory. In the weak-field formulation developed here with lattice spacing a , $\mu = 1/a$ must be below the Planck scale $\mu \ll m_{\text{P}}$, or equivalently $a \gg \ell_{\text{P}} \sim 10^{-20} \text{ fm}$. In principle, the effective theory includes terms proportional to R^2 and $R_{\mu\nu}^2$, though their contributions are small in the weak-field regime [10]. $\mathcal{L}_{\text{GR}}^{(2)}$ is quadratic in \mathbf{h} so is amenable to analytic perturbation theory. The approach developed here may offer a cross check of perturbative results [11, 12] and provide temperature dependence. The eventual goal is a combination of the spacetime and QCD vacua to permit two-way interaction.

2. Gauge fixing and discretization

GR has two physical degrees of freedom but symmetric \mathbf{h} has 10 components. Gauge fixing, for which we choose the harmonic gauge,

$$\partial_\mu h_{\mu\nu} - \frac{1}{2} \partial_\nu \text{tr} \mathbf{h} = 0, \quad (5)$$

¹Both κ and R have mass dimension 2. We input a value for the dimensionless quantity $a^2 \kappa$ and extract, e.g., the dimensionless quantity $a^2 R$ from the simulation. The value of $a^2 \kappa$ fixes the lattice spacing in the simulation.

eliminates four degrees of freedom. Four more are constrained by the contracted Bianchi identity, $\partial_\mu G_{\mu\nu} = 0$, written in terms of the Einstein tensor, $G_{\mu\nu} = R_{\mu\nu} - \frac{1}{2}Rg_{\mu\nu}$. As part of the Metropolis update algorithm Eq. (5) is used to fix diagonal entries of \mathbf{h} in terms of $h_{\mu\nu}$ with $\mu < \nu$.

A discrete (n^{th} order forward finite difference approximation, denoted f^n) and finite volume introduce discretization and finite volume systematic effects

$$\partial_\nu h_{\alpha\beta} = \delta_\nu^{(fn)} h_{\alpha\beta} + \mathcal{O}(a^n), \quad \int d^4x = a^4 \sum_x + \mathcal{O}(\text{FV}), \quad (6)$$

so that the lattice GR action is

$$S_{\text{GR}} = a^4 \sum_x \mathcal{L}_{\text{GR}}^{(2,fn)}(x) + \mathcal{O}(h^3, a^n, \text{FV}). \quad (7)$$

We use the same discretization to evaluate Eqs. (4) and (5).

3. Positive action conjecture

Provided $S_{\text{GR}} \geq 0$, the Markov chain gives snapshots of the dynamic spacetime vacuum with probability $p(\mathbf{h}) \propto e^{-S_{\text{GR}}(\mathbf{h})}$. $S_{\text{GR}} \geq 0$ is imposed via the positive action conjecture [5–8]: *all four-dimensional Riemannian asymptotically Euclidean manifolds have $S_{\text{GR}} \geq 0$, with $S_{\text{GR}} = 0$ if and only if the manifold is everywhere flat.* The proof [8] uses $R(x) \leq 0$ for all x and we require this to ensure a well-defined local probability density.

In analytic work, the positive action conjecture is enforced by adding a surface term to the action, e.g., the Gibbons-Hawking-York term,

$$S_{\text{GHY}} = 2\kappa \int_{\partial V} \sqrt{\det \hat{\mathbf{g}}} \left(\hat{g}_\nu^\mu \partial_\mu n^\nu + \frac{1}{2} \hat{g}^{\nu\rho} n^\mu \partial_\mu g_{\nu\rho} \right), \quad (8)$$

with n the unit normal to ∂V . $\delta(S_{\text{GR}} + S_{\text{GHY}}) = 0$ then ensures the metric induced on the boundary, $\hat{\mathbf{g}} = \mathbf{g}|_{\partial V}$, asymptotes to the flat space metric at infinity, ie. $\hat{\mathbf{g}} = \hat{\boldsymbol{\eta}} + \mathcal{O}(1/V)$, and that the Einstein field equations minimize the action. With the same discretization used to evaluate Eqs. (4) and (5), we instead explicitly impose

$$\mathbf{h}|_{\partial V} = \mathbf{0}, \quad n \cdot \partial \mathbf{h}|_{\partial V} = \mathbf{0} \quad (9)$$

on proposed values of \mathbf{h} on and near, as specified by the discretization, the boundary.

Perhaps because we use a discrete approximation of a Riemannian manifold, and/or because we impose positive action in finite volume, we see violations despite imposing Eq. (9). We additionally require that for proposed update $\mathbf{h} \rightarrow \tilde{\mathbf{h}}$, $R(\tilde{\mathbf{h}}) \leq 0$ everywhere, else the update is rejected. The frequency of violations is observed to decrease with increasing volume.

4. Metropolis updates

The merger of the positive action constraint, gauge fixing, and the Metropolis update algorithm is illustrated in Fig. 1. The size of random updates proposed for \mathbf{h} are fixed by the Planck length ℓ_P , ie. $h_{\alpha\beta} \rightarrow \tilde{h}_{\alpha\beta} = h_{\alpha\beta} + \epsilon_{\alpha\beta}$ with $\epsilon_{\alpha\beta}$ uniformly distributed in $-\ell_P/a \leq \epsilon_{\alpha\beta} \leq \ell_P/a$. Fig. 2 plots

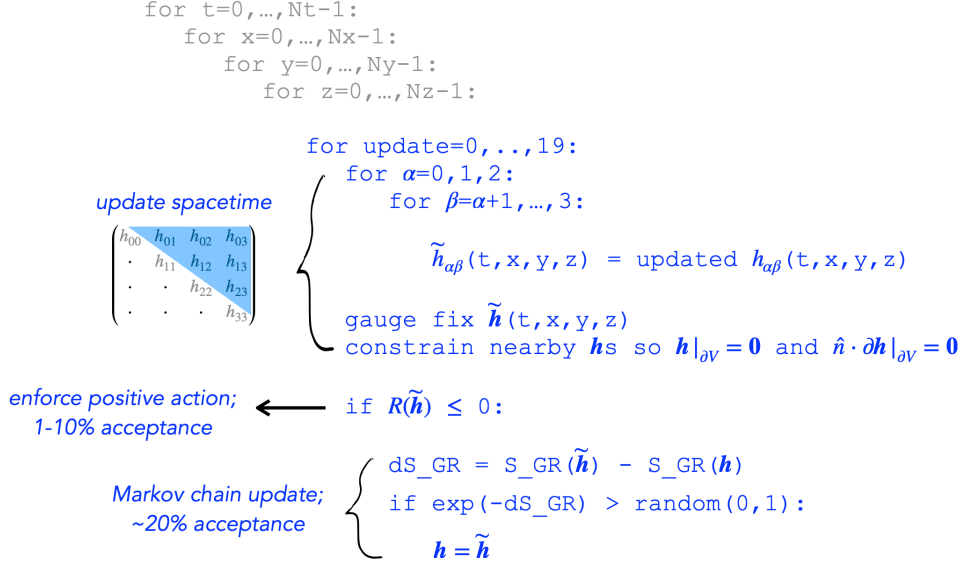


Figure 1: Sketch of a Metropolis sweep through the lattice, with 20 updates per spacetime point, including gauge fixing and the positive action conjecture. $R \leq 0$ is enforced for all spacetime points at which R changes as a result of a proposed update and the change in S_{GR} is evaluated over the same subset of spacetime points.

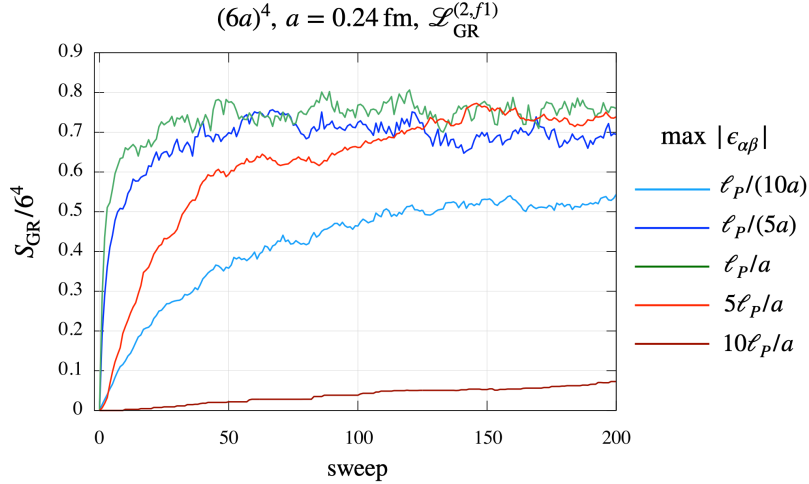


Figure 2: $S_{\text{GR}}/N_t N_s^3$ versus sweep for various choices of $\max |\epsilon_{\alpha\beta}|$ shows the Planck length results in the most efficient approach to thermalization. Larger updates result in lower acceptance rates while smaller updates have larger acceptance rates but require more sweeps to reach thermalization.

$S_{\text{GR}}/N_t N_s^3 = -a^4 \kappa \langle \sqrt{\det \mathbf{g}} R \rangle$, a proxy for the magnitude of the average curvature, demonstrating that the Planck length is the optimal choice for thermalization.

Ensembles generated are listed in Table 1, with parameters chosen to allow finite volume and temperature studies and a comparison of discretizations $f1$ and $f2$. The left panel of Fig. 3 shows a Markov chain of ensembles, demonstrating nonzero curvature of the spacetime vacuum, a consequence of the quantization of \mathbf{h} . The Metropolis algorithm suffers from significant autocorrelation, with autocorrelation lengths $\mathcal{O}(10^3)$ times longer than quenched lattice QCD with a similar setup. The right panel of of Fig. 3 shows the significant binning required to address autocorrelations.²

²Large autocorrelations result in low statistics, e.g., 13.9 binned measurements in Fig. 3. Errors are inflated by the student t distribution factor, $\sqrt{(N-1)/(N-3)}$ for N binned measurements, to partially address this.

ensemble	discretization	a/fm	N_t	T/MeV	N_s	L/fm	N_{cfg}	bin size
f1T137L072	$f1$	0.241	6	136.7	3^3	0.722	30481	2200
f1T137L144	$f1$	0.241	6	136.7	6^3	1.44	35812	3000
f1T137L217	$f1$	0.241	6	136.7	9^3	2.17	12449	800
f1T137L289	$f1$	0.241	6	136.7	12^3	2.89	15081	1800
f1T137L361	$f1$	0.241	6	136.7	15^3	3.61	6061	1500
f2T137L144	$f2$	0.241	6	136.7	6^3	1.44	19421	1400
f2T117L144	$f2$	0.241	7	117.1	6^3	1.44	32606	4000
f2T103L144	$f2$	0.241	8	102.5	6^3	1.44	22727	2000

Table 1: Ensembles with spacetime volume $aN_t (aN_s)^3$ generated for this study. Top panel ensembles use discretization $f1$ and have varying spatial volume while bottom panel ensembles use $f2$ and have varying temperature. The last column gives the bin size required to address autocorrelations.

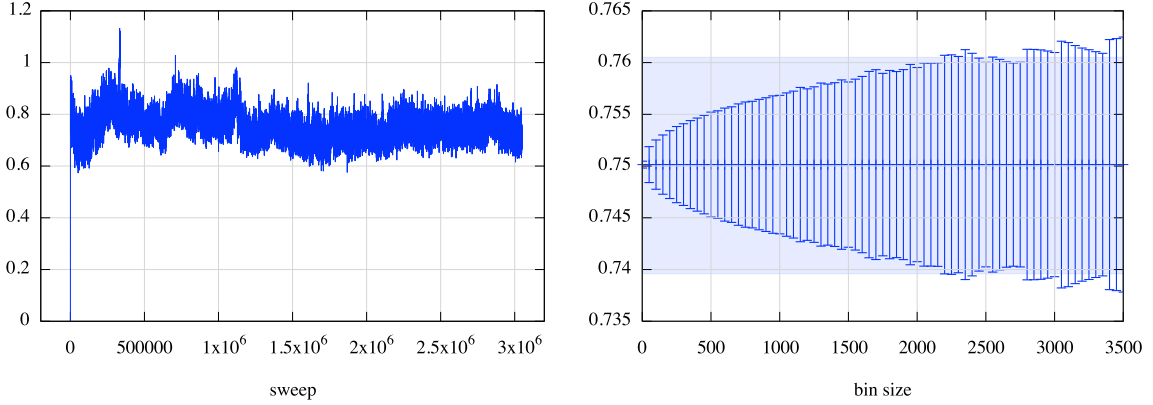


Figure 3: Left: The Markov chain for ensemble f1T137L072 is illustrated by plotting $S_{\text{GR}}/N_t N_s^3$ versus sweep. Right: A binning analysis of $S_{\text{GR}}/N_t N_s^3$ for saved configurations (every 100th sweep), with error band highlighted for a bin size of 2200.

5. Preliminary results, outlook, and summary

Though lattice spacings are only required to satisfy $a \gg \ell_p$, we choose a in anticipation of coupling spacetime and QCD. We are also generating vacuum spacetimes with zeptometer and nanometer scale lattice spacings to permit a study of scale dependence. Nonrenormalizability complicates the removal of discretization effects. In lieu of perturbatively running results at different lattice spacings to a common scale, we instead compare discretizations at fixed lattice spacing. Equilibrated ensembles f1T137L144 and f2T137L144 reveal a relative $\Delta S_{\text{GR}}^{(f1,f2)}$ of 13%. We are implementing the third order forward finite difference, $f3$, to see if $|\Delta S_{\text{GR}}^{(f2,f3)}| < \Delta S_{\text{GR}}^{(f1,f2)}$, which would provide further indication that discretization effects are under control.

The left panel of Fig. 4 shows results for $S_{\text{GR}}^{(2,f1)}/6N_s^3$ as a function of N_s , illustrating the feasibility of an infinite volume extrapolation. The only low energy scale in the simulation comes from the lattice spacing $\mu = 1/a$ (and perhaps the temperature, $T = 1/aN_t$, though within uncertainties the data do not require a second scale). Assuming exponentially decaying FV effects, the result of an unconstrained fit to $f(N_s) = f_\infty - f_\mu e^{-N_s}$ is shown overlaid on the data. The fit finds

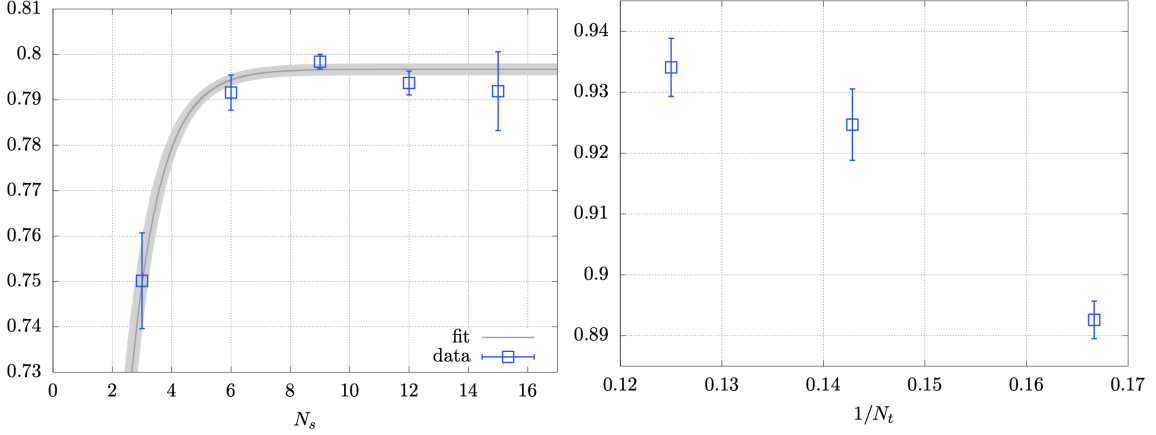


Figure 4: Left: Data for $S_{GR}^{(2,f^1)}/6N_s^3$ are plotted versus N_s for lattices with a temperature of $T = 136.7$ MeV. Overlaid is the result of a fit, discussed in the text, allowing an infinite volume extrapolation. Right: Data for $S_{GR}^{(2,f^2)}/N_t 6^3$ are plotted versus $1/N_t$ for lattices with a spatial extent of $L = 1.44$ fm.

$f_\infty = 0.7967(13)$ and $f_\mu = 0.95(21)$ with $\chi^2/\text{dof} = 3.3/3$. This f_∞ corresponds to an infinite volume average curvature, $\langle R_\infty \rangle = -3.1262(51) \times 10^{-3} \text{ m}^{-2}$.

The right panel of Fig. 4 shows data for $S_{GR}^{(2,f^2)}/N_t 6^3$ at three different temperatures. Classical GR is known to vary with temperature [13] and quantum GR effects have been found to decrease with temperature [14], consistent with our results.

Autocorrelations severely degrade the efficiency of data generation using the Metropolis algorithm with GR, significantly more so than with quenched QCD. We are implementing the Hamiltonian Monte Carlo update algorithm [15] in an attempt to address this.

We are currently evaluating components the Einstein tensor $G_{\mu\nu}$, which will allow a check of the contracted Bianchi identity, $\partial_\mu G_{\mu\nu} = 0$, and should allow for a calculation of the quantum vacuum contribution to the cosmological constant. We are also investigating calculating quantum corrections to the classical gravitational potential to allow comparison with analytic results [16].

Next, we plan to couple the dynamic vacua of spacetime and QCD to investigate their interaction. How these theories are coupled depends whether gravity is treated as a fundamentally classical or quantum theory [17].

Acknowledgments

Thanks to Salvatore Butera for many helpful discussions. Most of the ensembles were generated on the University of Glasgow’s Particle Physics Experiment group computing cluster.

References

- [1] G. ’tHooft and M.J.G. Veltman, *One loop divergencies in the theory of gravitation*, Ann. Inst. H. Poincaré Phys. Theor. A **20**, 69-94 (1974), http://www.numdam.org/item/AIHPA_1974__20_1_69_0/
- [2] E. Witten, *A Note On Complex Spacetime Metrics*, arXiv:2111.06514 [hep-th]

- [3] C. W. Misner, *Feynman quantization of general relativity*, Rev. Mod. Phys. **29**, 497-509 (1957), doi:[10.1103/RevModPhys.29.497](https://doi.org/10.1103/RevModPhys.29.497)
- [4] G. W. Gibbons and S. W. Hawking, *Euclidean quantum gravity*, Singapore: World Scientific (1993) 586 pages
- [5] J. W. York, Jr., *Role of conformal three geometry in the dynamics of gravitation*, Phys. Rev. Lett. **28**, 1082-1085 (1972), doi:[10.1103/PhysRevLett.28.1082](https://doi.org/10.1103/PhysRevLett.28.1082)
- [6] G. W. Gibbons, S. W. Hawking and M. J. Perry, *Path Integrals and the Indefiniteness of the Gravitational Action*, Nucl. Phys. B **138**, 141 (1978), doi:[10.1016/0550-3213\(78\)90161-X](https://doi.org/10.1016/0550-3213(78)90161-X)
- [7] G. W. Gibbons and C. N. Pope, *The Positive Action Conjecture and Asymptotically Euclidean Metrics in Quantum Gravity*, Commun. Math. Phys. **66**, 267 (1979), doi:[10.1007/BF01197188](https://doi.org/10.1007/BF01197188)
- [8] R. M. Schoen and S. T. Yau, *Proof Of The Positive Action Conjecture In Quantum Relativity*, Phys. Rev. Lett. **42**, 547 (1979), doi:[10.1103/PhysRevLett.42.547](https://doi.org/10.1103/PhysRevLett.42.547)
- [9] M. H. Goroff and A. Sagnotti, *Quantum gravity at two loops*, Phys. Lett. B **160**, 81-86 (1985), doi:[10.1016/0370-2693\(85\)91470-4](https://doi.org/10.1016/0370-2693(85)91470-4)
- [10] K. S. Stelle, *Classical gravity with higher derivatives*, Gen. Rel. Grav. **9**, 353-371 (1978), doi:[10.1007/BF00760427](https://doi.org/10.1007/BF00760427)
- [11] J. F. Donoghue, *Introduction to the effective field theory description of gravity*, arXiv:[gr-qc/9512024](https://arxiv.org/abs/gr-qc/9512024) [gr-qc]
- [12] C. P. Burgess, *Quantum gravity in everyday life: General relativity as an effective field theory*, Living Rev. Rel. **7**, 5-56 (2004), doi:[10.12942/lrr-2004-5](https://doi.org/10.12942/lrr-2004-5) [arXiv:[gr-qc/0311082](https://arxiv.org/abs/gr-qc/0311082) [gr-qc]]
- [13] R. C. Tolman, *On the Weight of Heat and Thermal Equilibrium in General Relativity*, Phys. Rev. **35**, 904-924 (1930), doi:[10.1103/PhysRev.35.904](https://doi.org/10.1103/PhysRev.35.904)
- [14] F. T. Brandt, J. Frenkel, D. G. C. McKeon and G. S. S. Sakoda, *Thermal quantum gravity in a general background gauge*, Phys. Rev. D **107**, no.8, 085020 (2023), doi:[10.1103/PhysRevD.107.085020](https://doi.org/10.1103/PhysRevD.107.085020) [arXiv:[2304.00166](https://arxiv.org/abs/2304.00166) [hep-th]]
- [15] S. Duane, A. D. Kennedy, B. J. Pendleton and D. Roweth, *Hybrid Monte Carlo*, Phys. Lett. B **195**, 216-222 (1987), doi:[10.1016/0370-2693\(87\)91197-X](https://doi.org/10.1016/0370-2693(87)91197-X)
- [16] J. F. Donoghue, *Leading quantum correction to the Newtonian potential*, Phys. Rev. Lett. **72**, 2996-2999 (1994), doi:[10.1103/PhysRevLett.72.2996](https://doi.org/10.1103/PhysRevLett.72.2996) [arXiv:[gr-qc/9311024](https://arxiv.org/abs/gr-qc/9311024) [gr-qc]]
- [17] J. Oppenheim, *A post-quantum theory of classical gravity?*, arXiv:[1811.03116](https://arxiv.org/abs/1811.03116) [hep-th]